Carbohydrate Research, 229 (1992) 57–74
Elsevier Science Publishers B.V., Amsterdam

Molecular and crystal structure of the regenerated form of (1→3)-α-D-mannan*

Toshifumi Yui[1], Kozo Ogawa[2] and Anatole Sarko

Chemistry Department, State University of New York, College of Environmental Science and Forestry, Syracuse, NY 13210 (USA)

(Received June 20th, 1991; accepted November 15th, 1991)

ABSTRACT

The crystal structure of the hydrated form of (1→3)-α-D-mannan, obtained by solid-state deacetylation of the partially *O*-acetylated mannan, was analyzed by combined X-ray diffraction and stereochemical-model refinement techniques. The structure crystallizes in a four-chain, monoclinic unit cell with parameters $a = 11.33$ Å, $b = 18.36$ Å, c (fiber repeat) $= 8.25$ Å, and $\gamma = 101.75°$, and the most probable space group is $P2_1$. In the most probable structure the chain-backbone conformation is a two-fold helix, but with all four O-6 rotational positions nonequivalent. The chains pack with antiparallel polarity and are connected by pairs of intermolecular hydrogen bonds that form an infinite, zig-zag sheet. There are 16 water molecules in the unit cell, generally embedded between the sheets in crystallographic positions, providing additional hydrogen bonding and establishing a three-dimensional hydrogen-bond network in the crystal structure. The reliability of the structure analysis is indicated by the X-ray residual $R'' = 0.281$, based on 98 *hkl* reflection intensities.

INTRODUCTION

Mannas are widely distributed in plant and microbial worlds, both as homo- and hetero-polysaccharides. In particular, the (1→3)-α-D-mannans are found as backbone chains of branched heteropolysaccharides in the fruiting bodies of some edible mushrooms. Examples are *Auricularia auricullajudae* (Kikurage)[1,2] and *Tremella fuciformis* Berk (Shirokikurage)[3,4], with the polysaccharide in both cases being D-glucurono-D-xylo-D-mannans, or (1→3)-α-D-mannan backbones branched with short segments of D-glucuronic acid and D-xylose. A linear (1→3)-α-D-mannan, containing one *O*-acetyl group at O-6 per two D-mannose residues, has been extracted from the fruiting body of *Dictyophora indusiata* Fish (Kinugasa-

Correspondence to: Dr. A Sarko, Chemistry Department, State University of New York, College of Environmental Science and Forestry, Syracuse, NY 132010, USA.

* Part 19 of the series: Packing Analysis of Carbohydrates and Polysaccharides.

[1] Faculty of Engineering, Miyazaki University, Miyazaki 889-21, Japan.

[2] Research Institute for Advanced Science and Technology, University of Osaka Prefecture, Osaka 593, Japan.

take)[5]. Variously linked mannose oligosaccharides are also important components of many glycoproteins.

Although considerable information has accumulated on the crystal structures and conformational characteristics of variously linked glucans, information in comparable detail for the mannans is not yet available. For this reason, we initiated a study of the crystalline characteristics of mannans, with the first report on (1→3)-α-D-mannan appearing[6] in 1986. Of interest were a detailed comparison of the crystal structure of this mannan with the corresponding glucan[7], and in particular, the hydrate structure of mannan as opposed to the anhydrous form of the glucan.

Many polysaccharides have been observed to crystallize in a hydrate form with water molecules either in crystallographic positions or as statistically random components of the crystal structure. All such water molecules contribute to the hydrogen bonding of the polysaccharides and are thus important components of the structure. In some cases, such as amylose (starch)[8,9] and (1→3)-β-D-glucan[10], hydrate forms are found in the native state. In other cases, hydration has been found to occur in intermediate stages, as for example, during the mercerization of cellulose[11]. Therefore, a detailed characterization of the hydrate structure of polysaccharides could provide information pertaining to biological functions or mechanisms of structural transformations for these molecules.

In a previous report[6], we described the successful crystallization of a (1→3)-α-D-mannan obtained by solid-state deacetylation of a solution-generated film. The X-ray data suggested a two-fold helical structure similar to that of (1→3)-α-D-glucan[7]. A hydrated structure was also suggested, perhaps involving up to two water molecules for each mannose residue. In the present report, we describe the detailed structure analysis and refinement of this mannan hydrate.

EXPERIMENTAL

Sample preparation.—A partially *O*-acetylated linear (1→3)-α-D-mannan (mol wt 6.2×10^5) had been prepared by extraction with aq 70% EtOH from the fruiting body of *Dictyophora indusiata* Fish. It was soluble in Me_2SO and yielded a flexible film upon drying of a 23 mg/ml solution. A strip of the film was stretched in aq 75% MeOH at 60°, followed by deacetylation in 2 M methanolic NaOMe overnight at room temperature, while keeping the film clamped at constant length. The stretched, deacetylated sample was annealed in aq 70% isopropyl alcohol at 180° or higher, in order to improve crystallinity.

The density of the samples was measured by flotation in a CCl_4–*m*-xylene mixture.

X-ray diffraction measurements. —X-ray diffraction patterns were recorded in a sealed flat-film camera, using Cu$K\alpha$ radiation and Fuji RX X-ray film. A well-resolved X-ray fiber pattern, shown in Fig. 1, was obtained at high relative humidity in a helium atmosphere.

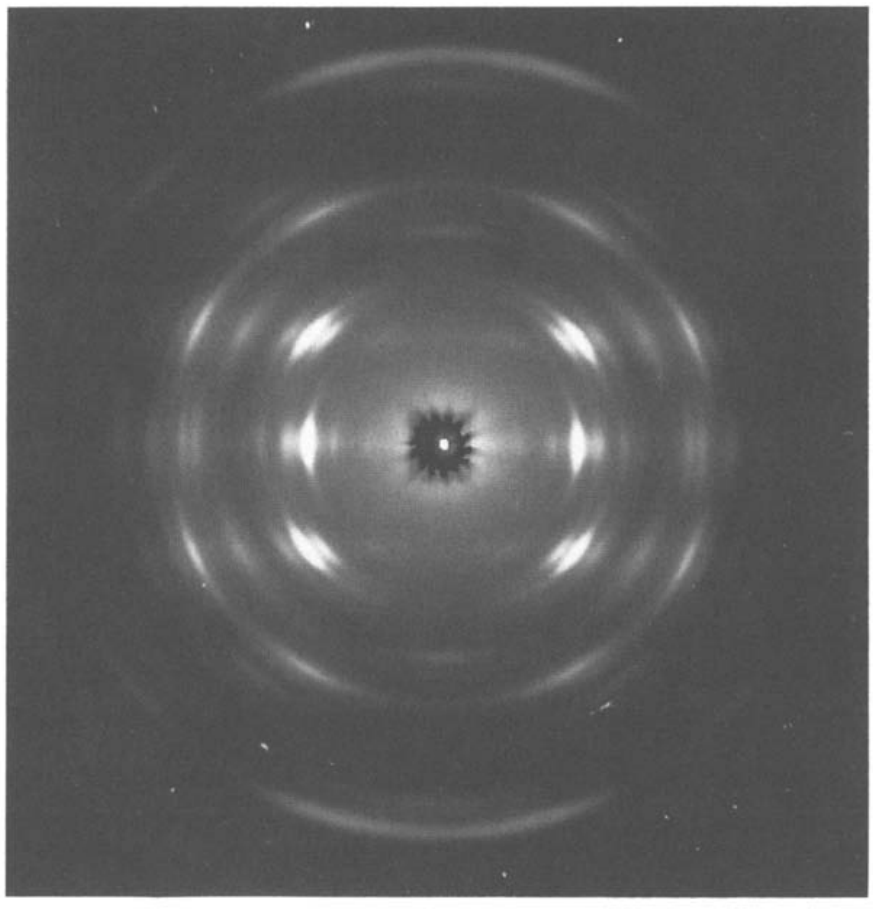

Fig. 1. The X-ray fiber pattern of (1→3)-α-D-mannan hydrate. The fiber axis is vertical.

The unit-cell parameters were determined by least-squares refinement with d spacings measured for 47 diffraction peaks. Relative intensities of the peaks were obtained from radial tracings recorded with a Joyce–Loebl Mark IIIc microdensitometer. The areas under the tracings were resolved, as far as possible, into individual intensities with either a least-squares curve resolution program[12] or visual estimation, followed by corrections[13] for Lorentz and polarization factors, a temperature factor[14], and arcing of the reflections. The square roots of the corrected intensities constituted the relative, observed structure factor amplitudes. Unobserved reflections were assigned relative intensities of one-half of the minimum observable value in the corresponding region of the diffraction angle.

Structure determination and refinement. —The analysis and refinement of the structure were carried out with the refinement program[15] PS79. The details of the theory and strategy of this refinement program have been previously described[16]. Briefly, the following procedures were used.

The stereochemical characteristics of the structure were refined by minimizing the nonbonded repulsion energy:

$$E = \sum_{\substack{i=1 \\ j=1}} w_{ij}\left(d_{ij} - d_{ij}^0\right)^2 \qquad (1)$$

where d_{ij} is the distance between nonbonded atoms i and j, d_{ij}^0 is the corresponding equilibrium distance, and w_{ij} is the weight assigned to the ijth contact in the summation. For chain conformation refinement, the contacts were those of an

TABLE I

Comparison of calculated and observed *d* spacings (Å)

h	*k*	*l*	Calcd	Obsd	*h*	*k*	*l*	Calcd	Obsd
1	0	0	11.093	11.16	0	0	2	4.125	4.16
1	−2	0	7.804	7.81	1	0	2	3.866	3.89
1	2	0	6.377	6.38	1	−1	2	3.836	
2	−1	0	5.633	5.61	1	2	2	3.464	3.46
2	0	0	5.546		1	−3	2	3.359	
1	3	0	4.873	4.86	2	−1	2	3.328	3.33
1	−4	0	4.496		2	0	2	3.310	
0	4	0	4.494	4.43	1	3	2	3.148	3.15
2	3	0	3.711		2	2	2	2.990	2.99
3	0	0	3.698		3	−1	2	2.786	
3	−2	0	3.694	3.68	2	3	2	2.759	2.77
1	−5	0	3.645		3	0	2	2.753	
3	1	0	3.484	3.50	3	−2	2	2.752	
3	−3	0	3.479		3	1	2	2.662	2.67
1	5	0	3.232		3	−3	2	2.660	
3	2	0	3.198	3.20	1	5	2	2.544	
3	−4	0	3.192		3	2	2	2.527	
2	4	0	3.188		3	−4	2	2.524	
3	3	0	2.894		2	4	2	2.523	2.52
2	−6	0	2.894	2.92	4	−5	2	2.107	
3	−5	0	2.888		2	6	2	2.098	2.09
4	−5	0	2.450	2.45	1	7	2	2.072	
2	6	0	2.437		4	−7	2	1.879	
5	1	0	2.149		5	−5	2	1.863	1.86
3	6	0	2.126	2.13	5	2	2	1.842	
3	−8	0	2.121		5	3	2	1.767	
1	8	0	2.120		4	−8	2	1.764	
4	−7	0	2.111		2	8	2	1.762	1.76
0	1	1	7.498	7.70	3	7	2	1.750	
1	0	1	6.620	6.82	3	−9	2	1.748	
1	−2	1	5.669	5.61	1	0	3	2.669	2.67
1	2	1	5.045	5.05	1	−1	3	2.659	
2	−1	1	4.652	4.63	1	2	3	2.525	2.52
2	0	1	4.603		0	3	3	2.499	
1	−4	1	3.948		1	3	3	2.395	2.38
0	4	1	3.946	3.92	2	−3	3	2.355	
2	3	1	3.384	3.38	1	−5	3	2.195	
3	0	1	3.374		3	1	3	2.159	
3	−2	1	3.372		3	−3	3	2.157	
3	1	1	3.210	3.23	4	−5	3	1.829	
3	−3	1	3.206		2	6	3	1.824	
1	5	1	3.010	3.00	1	7	3	1.807	1.81
3	2	1	2.982		3	5	3	1.786	
3	−4	1	2.977						
2	4	1	2.974		0	0	4	2.062	2.06
0	6	1	2.816	2.82	1	−2	4	1.994	
3	−6	1	2.481		1	2	4	1.962	1.97
0	7	1	2.452	2.46	0	3	4	1.950	
4	−5	1	2.349		1	3	4	1.899	
2	6	1	2.337	2.31	2	−3	4	1.879	1.88

TABLE I (continued)

h	k	l	Calcd	Obsd	h	k	l	Calcd	Obsd
5	−2	1	2.183		1	−4	4	1.875	
5	−1	1	2.178		0	4	4	1.874	
2	−8	1	2.169	2.17	2	2	4	1.863	
0	8	1	2.168		2	−4	4	1.823	
5	−3	1	2.156	1	4	4	1.823		
5	1	1	2.080	3	−1	4	1.810	1.81	
3	6	1	2.058	2.06		2	3	4	1.803
3	−8	1	2.055		3	0	4	1.801	
1	8	1	2.053		3	−2	4	1.801	
4	−7	1	2.045		1	−5	4	1.795	
					0	5	4	1.789	

isolated chain only. Subsequently, interactions between the chains were included for the chain packing refinement.

The X-ray refinement was carried out with structure-factor amplitudes, by minimizing the weighted crystallographic residual:

$$R'' = \left[\sum w \| F_o | - | F_c \|^2 / \sum w | F_o |^2\right]^{1/2} \quad (2)$$

The unweighted residual:

$$R = \sum \| F_o | - | F_c \| / \sum | F_o | \quad (3)$$

was also calculated. In these equations, $|F_o|$ and $|F_c|$ are the observed and calculated structure factor amplitudes, respectively, and the weights w are assigned at 1.0 for the observed reflections, 0.5 for the unobserved reflections when $|F_c| > |F_o|$, and 0 for the latter when $|F_c| < |F_o|$. The weighted residual was used exclusively throughout the structure refinement because of a considerable number of unobserved reflections present in the X-ray data set.

During the final stages of the refinement the stereochemically constrained refinement function:

$$\Phi = fR'' + (1 - f)E \quad (4)$$

was minimized, where E is the complete stereochemical function incorporating all bond length, bond angle, and torsion angle strains, as well as the nonbonded repulsion term of eq *1* (see, for example, eq *1* in ref. 16), R'' is the X-ray residual of eq *2* (expressed in percent) and f is a fractional weight so chosen that both terms contribute approximately equally to the whole equation.

During the final refinement, the components B_x, B_y, and B_z of an anisotropic temperature factor[17] were included as variables, partially to correct for unequal X-ray scaling factors and for the effects of corrections applied isotropically to the observed intensities.

RESULTS AND DISCUSSION

Unit-cell parameters. —In the previous paper[6], we concluded that (1→3)-α-D-mannan crystallized in a monoclinic unit cell that contained eight mannose residues (i.e., four chains) and 16 water molecules. The previously reported unit-cell parameters were re-refined because of re-assignments of several reflections, which resulted in new unit-cell parameters $a = 11.33$ Å, $b = 18.36$ Å, c (fiber repeat) = 8.25 Å, and $\gamma = 101.75°$. The new calculated density, $\rho_{calc} = 1.57$ g/cm^3, was in good agreement with the experimental value, $\rho_{exp} = 1.50$ g/cm^3. A comparison of the observed and calculated d spacings is shown in Table I.

The X-ray diagram exhibited two meridional reflections, on the 2nd and 4th layer lines, which suggested the presence of a two-fold screw axis along the c-axis of the unit cell. Consequently, a two-fold helical conformation, similar to that found in the (1→3)-α-D-glucan[7], was assumed as a starting model, but the space group $P2_1$ was initially not assumed.

Chain conformation. —The initial coordinates of α-D-mannan were based on the standard α-glucopyranose residue of Arnott and Scott[18], except for the geometry of the O-2 atom. The position of the latter was defined by setting the conformation angle O-3–C-3–C-2–O-2 at −55.5°, based on the crystal data of methyl α-D-mannopyranoside[19], while the bond length C-2–O-2 and the bond angle C-3–C-2–O-2 remained at their standard values (1.423 Å and 110.8°, respectively). This combination of the internal coordinates of the O-2 atom resulted in minimal deviation of the bond angle C-1–C-2–O-2 (107.5°) from its standard value (109.3°). The length of the *virtual bond*, a vector joining successive glycosidic bridge oxygens, was 4.232 Å for this residue.

The conformational analysis of the chain was carried out under the constraint of two-fold screw symmetry. All three most probable O-6 rotational positions (*gg*, *gt*, and *tg*[20]) were investigated, but no clear differences could be found among the three resulting models in either the chain conformation or its energy, indicating that the O-6 position had little effect on the isolated chain structure. Hence the refined chain conformation of the O-6-*gg* model was used as the initial structure in the subsequent chain-packing refinement and O-6-*gt* and *tg* models were obtained simply by rotating the O-6 atom to the corresponding positions. The glycosidic bridge angle of this, the most probable chain model was 119.9°, nearly identical with the angle for the (1→3)-α-D-glucan (119.5° after the chain conformation refinement). No intramolecular hydrogen bonds appeared. (It should be noted that only the O-2 · · · O-4′ intramolecular hydrogen bond is present in the (1→3)-α-D-glucan chain and that the same bond is not possible in mannan due to the axial disposition of the O-2 atom.)

Chain packing. —Because of the presence of water molecules in the structure the chain packing in the unit cell was not tight and had to be solved entirely by X-ray refinement, with little help from stereochemical packing analysis. It proceeded in two steps. In the first step, the refinement was carried out with the

equatorial data only, using 21 *hk0* reflection intensities, in order to determine the translational and rotational positions of the chains in the *ab* plane and the chain packing polarities. This was followed, in the second step, by the introduction of the chain translational position along the *c* (fiber) axis as a variable, and the refinement with 55 *hkl* reflection intensities ($l = 0$–2), so that the three-dimensional structure could be determined. During the refinement in the first step, models in both $P1$ and $P2_1$ space groups were tested, and as it turned out, the resulting structures for both models were nearly equivalent. Since the $P2_1$ structure, having only four independent residues, involved fewer refinement variables than the $P1$ structure, only the $P2_1$ structure was advanced to the second step. (The rationale for this choice became more evident later as water molecules were added.) Although the resulting three-dimensional structure was still tested further by eliminating the two-fold screw axis (in effect, reducing the symmetry to $P1$), no chains were found to move away from the original $P2_1$ symmetry positions. In this structure, a two-fold screw axis does not coincide with the chain axis, residing instead between the chains. The mannose dimer was, consequently, the crystallographic repeat unit. Similar packing features were proposed for the crystal structure of (1 → 3)-α-D-glucan[7]. In the following refinement stages, however, a molecular two-fold screw axis was maintained in the mannan chain.

During these refinements, all $P2_1$ models were further tested using the water-weighted atomic scattering factors. The use of the latter factors is based on the assumption that the volume of the unit cell is filled with an electron gas whose density is equal to the mean electron density of water. The water-weighted scattering factors have been successfully used with other water-containing structures[21–24] in which water molecules were generally not occupying crystallographically defined positions.

As shown in Table II, the use of water-weighted scattering factors clearly reduced the R''-factors after the first refinement step. However, their use became much less effective when three-dimensional X-ray data were added in the second step. In addition, these R''-factors were judged to be still too high for a reasonable

TABLE II

Results of chain-packing refinement for the $P2_1$ structure

O-6 Model	R'' With ordinary Atomic scattering factors	R'' With H_2O weighted
1st step: 21 *hk0* reflection intensities		
gg	0.302	0.214
gt	0.267	0.210
tg	0.386	0.276
2nd step: 55 *hkl* reflection intensities		
gg	0.372	0.363
gt	0.382	0.387
tg	0.401	0.388

structure, even though not all variables had been refined at this stage. Identical behavior had been observed earlier in the structure analysis of (1→3)-β-D-glucan hydrate[21] where the structure was ultimately solved by placing water molecules at crystallographic positions in the unit cell. Consequently, the possibility of water molecules occupying preferred positions in the mannan structure was investigated next.

Placement of water molecules. —On the basis of crystalline density the structure was likely to contain 16 water molecules, or eight independent water molecules under $P2_1$ symmetry. The strategy which had been successfully used in the analysis of alkali-cellulose structures[11] was employed to locate these water molecules. Initially, the water positions were determined in the *ab*-projection using 21 *hk0* reflection intensities. The *ab*-plane corresponding to the asymmetric unit was divided into small rectangular regions (1.4×1.5 Å^2), and the x–y coordinates of a single water molecule (as oxygen) were refined in each such region in turn. This produced an R''-factor map (shown in Fig. 2) which clearly indicated the positions of four water molecules. The z-coordinate of each water molecule was then quickly refined with 40 *hkl* reflection intensities ($l = 0, 1$), starting from several trial positions. The next four water molecules were located in the same manner, but now starting with the structure containing the four water molecules previously found. The hydrate structure thus obtained was subjected to a further refinement against 55 *hkl* reflection intensities where the variables were chain rotations and translations, the residue rotation about the *virtual bond*, O-6 rotations, and the x, y, z translations of all water molecules.

As expected, introducing the water molecules into the crystal structure lowered the R''-factor to about 0.2. However, the water molecules tended to move too close to the mannose residues during this refinement, with some of the contacts becoming unreasonably short. The results obtained with this unconstrained X-ray refinement clearly showed that the most probable structure determined by X-ray refinement did not completely coincide with that residing in a stereochemical energy minimum. This is not surprising considering the small X-ray data set and the fact that each individual water molecule was allowed to move freely, without any stereochemical constraints, unlike the residue atoms whose motions must be correlated with those of other atoms in the residue. In order to introduce realistic stereochemical constraints on the water molecules, their subsequent refinement was carried out first by a pure stereochemical refinement (eq *1*), followed by a stereochemically constrained X-ray refinement (eq *4*). As a result, reasonable packing structures were obtained at the expense of an approximately 0.10 increase in the R''-factor.

Table III summarizes the results obtained for the three O-6 rotation models containing various amounts of water. The results with water-weighted structure factors are shown for comparison. (It should be noted that the structures containing no water were obtained by X-ray refinement only, while the others were obtained by combined X-ray-stereochemical refinement.) The structure containing

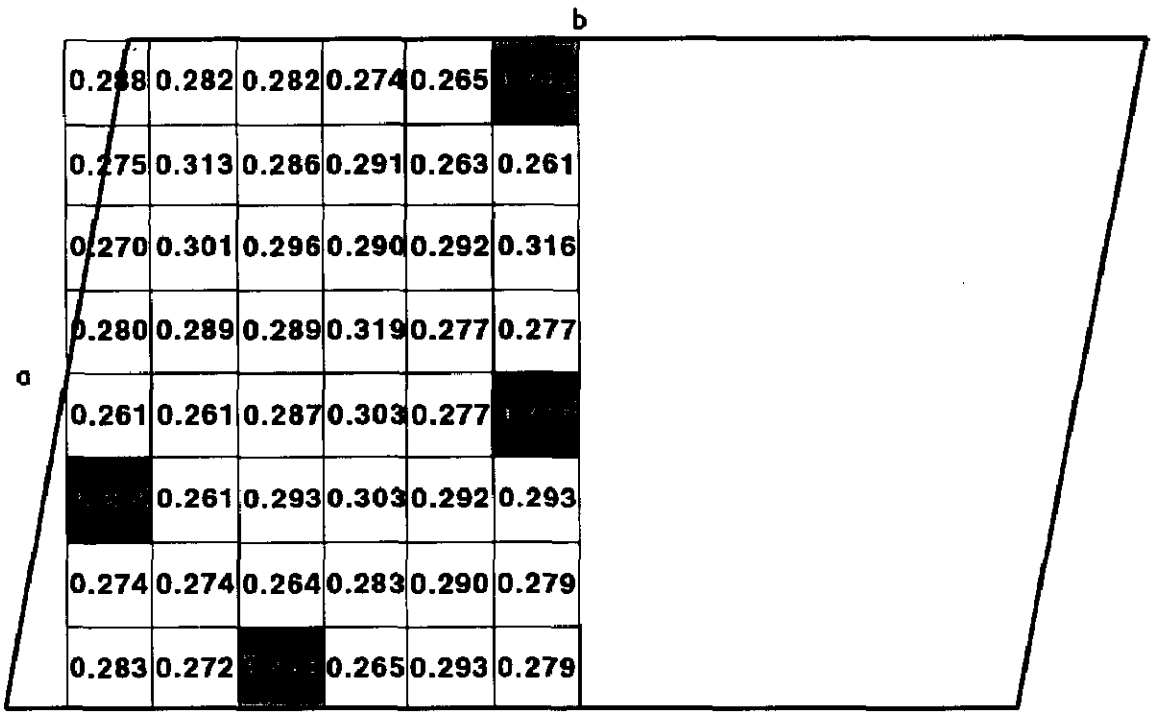

Fig. 2. *R″*-factor maps of the *ab*-plane of the structure (O-6-*gt* model) with no water (top) and with one water each placed at the indicated positions (bottom). Both maps show four minima of the *R″*-factor, illustrated by shaded rectangulars. (The other half of the projection is related to the first by symmetry operation.)

eight water molecules was also tested with water-weighted scattering factors on the assumption that some of the water molecules could be in noncrystallographic positions, as was observed in the case of the (1→3)-β-D-glucan hydrate structure[21]. It is clear from the results that the structures with all 16 waters in crystallographically defined positions were the most probable ones. The O-6-*gt* structure was preferred over other models on the basis of the lowest *R″*-factor.

The nonequivalent O-6 models. —It became apparent from the distribution of water molecules which had resulted from pure X-ray refinement that the water molecules were not subject to two-fold helix symmetry of the chain. This suggested that nonequivalent rotational positions of O-6 atoms would also be likely, providing increased hydrogen bonding for the water molecules. Accordingly, an investiga-

TABLE III

Results of refinement of various hydrate structures

O-6 Model (chain 1/chain 2)	No. of H_2O's[a]	Atomic scattering factors	R''[b]	E[c]
Equivalent models:				
gg	0	H_2O-wtd	0.361	37
gt	0	H_2O-wtd	0.385	43
tg	0	H_2O-wtd	–	–[d]
gt	8	H_2O-wtd	0.396	71
gt	12	ordinary	0.343	83
gg	16	ordinary	0.336	118
gt	16	ordinary	0.309	120
tg	16	ordinary	0.344	97
Nonequivalent models:				
gt-gt / gg-gg	16	ordinary	0.299	127
tg-gt / gg-gg	16	ordinary	0.291	133
tg-gg / gg-gg	16	ordinary	0.281	127

[a] Per unit cell. [b] With 55 *hkl* reflection intensities ($l = 0$-2). [c] From eq *1*, in arbitrary units. [d] An O-6-*tg* model could not be obtained since the O-6 atom rotated away from the *tg* position nearly reaching the *gg* position during refinement.

tion of nonequivalent O-6 models was made, starting with 30 models, each of which had various combinations of O-6 positions. At first, no water molecules were included. The best 12 models were selected on the basis of their R''-factors and were followed up by refinement with all 16 water molecules included. Finally, the best three models were subjected to a combined X-ray–stereochemical refinement of water positions as was done with previous models. The results are listed in the lower part of Table III.

Compared with equivalent O-6 models, the nonequivalent O-6 models all showed slightly lower R''-factors without significantly increased packing energies. In addition, these models exhibited reasonable features of hydrate structure. The water molecules were distributed more evenly within the unit cell allowing most water and mannose oxygens to participate in hydrogen bonding.

Among all of these models, the distribution of water molecules was generally similar. (Of the equivalent O-6 models, only the O-6-*gt* model, having the best R''-factor, also showed a similar water distribution.) This consistency in the results for water distributions, coupled with a preference in the R''-factors, was considered to be good evidence for the support of hydrate structure based on nonequivalent O-6 positions. Consequently, all three nonequivalent O-6 models were selected for final refinement.

Hydrogen bonding and the final structure. —The final stage of refinement was carried out using the combined stereochemical X-ray equation (eq *4*). The variables to be refined were chain rotations and translations, all four O-6 rotations, residue rotation about the *virtual bond*, and the three-dimensional translations of

TABLE IV

Characteristics of three nonequivalent O-6 models

R^a	R''^a	B (isotropic)	E	No. of H-bonds[b]	No. of contacts[b]
1. O-6-*gt-gt / gg-gg* model:					
0.400	0.354	8.74	74	28	8
2. O-6-*tg-gt / gg-gg* model:					
0.422	0.337	10.9	75	26	7
3. O-6-*tg-gg / gg-gg* model:					
0.400	0.337	13.4	55	26	5
0.380	0.323	$B_x = 0.00$			
		$B_y = 17.8$			
		$B_z = 18.3$[c]			
After intensity correction:					
0.278	0.220	$B_x = 0.402$			
		$B_y = 15.0$			
		$B_z = 17.1$[c]			

[a] With 62 *hkl* reflection intensities ($l = 0$–3). [b] In asymmetric unit. [c] Components of anisotropic temperature factor, see text.

eight independent water molecules. During the refinement, all appropriate oxygen–oxygen distances less than 3.1 Å were considered to be hydrogen bonds. (The hydrogen-bond function that was used had a minimum energy[16] at a distance of 2.8 Å.) This procedure immediately improved the short-contacts picture, since most previously considered short contacts were between oxygen atoms. Subsequently, the X-ray data from the 3rd layer (7 *hk3*) were added and a temperature factor was included as a variable. The resulting characteristics of the three models are listed in Table IV, showing a slight preference for the O-6-*tg-gg / gg-gg* model, both in *R*-factors and the packing energy, as well as in the smallest number of short contacts. This structure was, therefore, selected as the most probable crystal structure for the (1→3)-α-D-mannan hydrate. Refining it further with anisotropic temperature factors against all 62 *hkl* ($l = 0$–3) reflection intensities reduced the *R''*-factor to 0.323 (compare Table IV).

Throughout all stages of the refinement, it had been noticed that some overlapping observed and unobserved reflections exhibited a consistent reversal of observed and calculated amplitudes ($|F_o|$ and $|F_c|$). The values of $|F_c|$ for the observed reflections were found to be smaller than the corresponding values of $|F_o|$, and the neighboring unobserved reflections showed larger values of $|F_c|$ than those that had been assigned to $|F_o|$. This suggested that the reflections originally considered to be unobserved were, in fact, contributing their intensities to the adjacent observed reflections. Checking the peak positions of the unobserved reflections on the densitometer tracings indeed showed that they fell within the observed peak envelopes. After a recombination of the four sets of the reflections in question (two on the 1st layer and one each on the 2nd and 3rd

layers), a few cycles of refinement with the corrected X-ray data immediately reduced the R''-factor to 0.220 (see Table IV). The improvement was remarkable in view of the fact that only four out of a total of 62 reflection intensities were subject to the correction.

For the final few runs of the refinement, the X-ray data from the external regions of the diffractogram were added. These X-ray data had not been included throughout the preceding refinement because they contained many unobserved reflections. The final structure of the O-6-*tg-gg / gg-gg* model, refined with 98 *hkl* reflection intensities, gave an R''-factor of 0.281 (with anisotropic temperature factor). It should be noted that despite the correction of the X-ray data, little change in the structure resulted after the full refinement, in comparison with results obtained with uncorrected X-ray data set of 62 *hkls*. The details of the final structure are described in Table V, its hydrogen bonds are shown in Table VI, and

TABLE V

Major characteristics of the final structure

Parameter	Chain 1	Chain 2
Position of chain axis (x, y, z in Å)[a]	2.909, 2.133, 0.000	2.833, 11.274, 2.375
Rotational position of chain[b]	5.2°	126.4°
Glycosidic bridge angles at O-3	118.6°	
Conformation angles[c] ϕ, ψ	−48.9°, −3.0°	
O-6 Conformation angles[d]	O-6_1 −148.4° O-6_2 −41.8°	O-6_3 −64.3° O-6_4 −64.4°
Packing energy (E) (per residue, arbitrary units)	13.1	
Short contacts[e] and lengths (in Å)	H-6a_4 O_w-3 H-6b_1 O_w-7′ O-2_1 O_w-8	2.18 2.13 2.48
X-Ray residuals[f]: R R''	0.345 0.281	
Components of temperature factor: B_x, B_y, B_z	13.9, 11.2, 15.4	

[a] Measured from unit-cell origin, see Fig. 3. [b] 0° Position is when O-3 is at 0, $-y$, for a chain that is at unit cell origin. Positive rotation is clockwise looking down helix axis. [c] $\phi = 0°$ when bond sequence H-1_1–C-1_1–O-3_2–C-3_2 is *cis*; $\psi = 0°$ when bond sequence C-1_1–O-3_2–C-3_2–H-3_2 is *cis*; positive angle is for the far bond clockwise relative to the near bond. [d] Conformation angle O-5–C-5–C-6–O-6 is 0° when *cis*; $gg = -60°$, $gt = 60°$, $tg = 180°$. [e] Prime indicates an equivalent position at: $-x$, $-y$, $0.5+z$. [f] With 98 *hkl* reflection intensities (l = 0-3) including those from the furthest regions of the diffractogram.

TABLE VI

Hydrogen bonds of the final structure

A. Interchain hydrogen bonds	
Hydrogen bond[a]	Length (Å)
O-4_1 · · · O-$2_{2'}$	2.93
O-6_2 · · · O-$4_{3'}$	2.70
O-2_2 · · · O-$6_{3'}$	2.70
O-4_4 · · · O-$6_{4'}$	2.88

B. Distribution of hydrogen bonds involving water			
Water molecule		No. of bonds	
O_w-1	O_w-5	2	2
O_w-2	O_w-6	3	4
O_w-3	O_w-7	3	4
O_w-4	O_w-8	3	4

[a] Prime indicates an equivalent position at: $-x, -y, 0.5+z$.

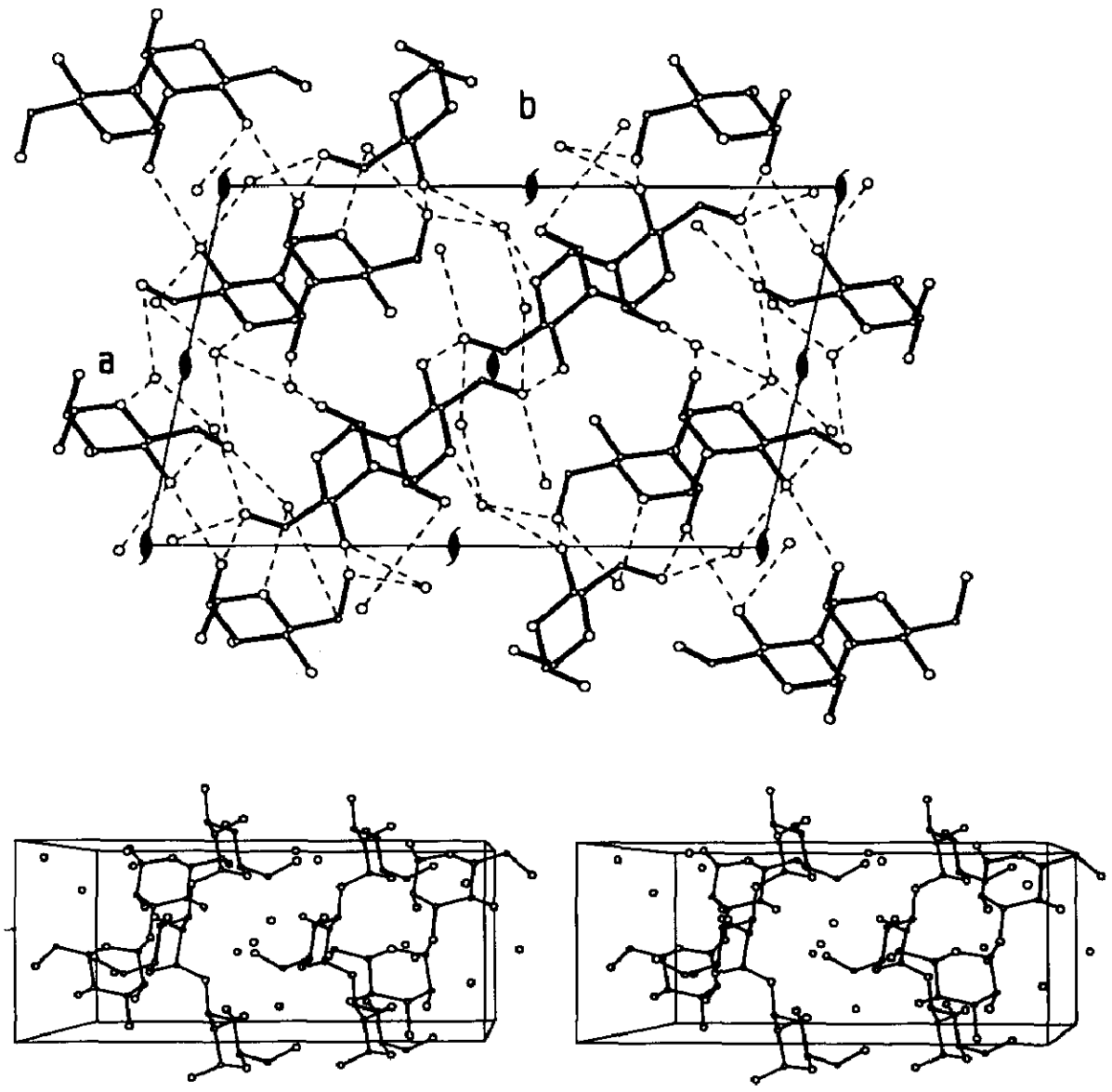

Fig. 3. Projections of the structure on *ab* plane. All hydrogen atoms have been omitted and hydrogen bonds are shown as dashed lines (top). Stereoviews of the structure on *bc* plane (bottom).

TABLE VII

Cartesian atomic coordinates of final structure (Å)

Atom	x	y	z
Helix 1			
O-4_1	1.922	−0.696	1.407
C-4_1	3.063	0.063	1.798
C-1_1	4.131	2.134	3.502
C-3_1	2.882	1.527	1.422
C-2_1	4.009	2.367	2.002
C-5_1	3.247	−0.076	3.305
O-5_1	4.332	0.755	3.743
O-2_1	5.255	2.017	1.412
O-3_1	2.865	1.661	0.000
C-6_1	3.579	−1.492	3.725
O-6_1	3.052	−2.453	2.813
H-1_1	4.954	2.672	3.869
H-2_1	3.813	3.383	1.823
H-3_1	1.967	1.868	1.809
H-4_1	3.913	−0.316	1.311
H-5_1	2.365	0.228	3.788
H-6a$_1$	3.194	−1.672	4.686
H-6b$_1$	4.623	−1.596	3.757
O-4_2	3.895	4.963	5.532
C-4_2	2.754	4.204	5.923
C-1_2	1.686	2.133	7.627
C-3_2	2.935	2.740	5.547
C-2_2	1.808	1.899	6.127
C-5_2	2.570	4.342	7.430
O-5_2	1.485	3.511	7.868
O-2_2	0.562	2.250	5.537
O-3_2	2.952	2.605	4.125
C-6_2	2.238	5.758	7.850
O-6_2	0.864	6.068	7.627
H-1_2	0.863	1.595	7.994
H-2_2	2.004	0.883	5.948
H-3_2	3.850	2.398	5.934
H-4_2	1.904	4.582	5.436
H-5_2	3.452	4.039	7.913
H-6a$_2$	2.841	6.433	7.317
H-6b$_2$	2.443	5.861	8.875
Helix 2			
O-4_3	0.062	12.414	0.968
C-4_3	1.388	12.764	0.577
C-1_3	3.645	12.188	−1.127
C-3_3	2.362	11.657	0.952
C-2_3	3.739	11.942	0.373
C-5_3	1.406	12.994	−0.930
O-5_3	2.748	13.253	−1.368
O-2_3	4.304	13.106	0.963
O-3_3	2.452	11.555	2.375
C-6_3	0.568	14.182	−1.351
O-6_3	0.976	15.378	−0.689
H-1_3	4.594	12.447	−1.494

TABLE VII (continued)

Atom	x	y	z
Helix 2			
H-2_3	4.368	11.121	0.552
H-3_3	2.010	10.746	0.566
H-4_3	1.669	13.651	1.064
H-5_3	1.047	12.133	−1.413
H-$6a_3$	−0.443	13.991	−1.138
H-$6b_3$	0.673	14.318	−2.386
O-4_4	5.604	10.134	−3.157
C-4_4	4.279	9.784	−3.548
C-1_4	2.021	10.360	−5.252
C-3_4	3.305	10.892	−3.173
C-2_4	1.928	10.607	−3.752
C-5_4	4.261	9.555	−5.055
O-5_4	2.919	9.295	−5.493
O-2_4	1.363	9.442	−3.162
O-3_4	3.215	10.993	−1.750
C-6_4	5.099	8.366	−5.476
O-6_4	4.693	7.171	−4.812
H-1_4	1.072	10.102	−5.619
H-2_4	1.298	11.428	−3.573
H-3_4	3.657	11.802	−3.559
H-4_4	3.998	8.897	−3.061
H-5_4	4.619	10.416	−5.538
H-$6a_4$	6.110	8.558	−5.265
H-$6b_4$	4.992	8.229	−6.511
Water molecules			
O_w-1	1.919	6.437	3.431
O_w-2	3.598	−2.049	7.812
O_w-3	7.347	7.078	3.995
O_w-4	9.912	1.963	7.858
O_w-5	−0.146	0.796	2.380
O_w-6	1.255	8.329	0.817
O_w-7	5.145	−0.251	6.275
O_w-8	6.221	1.994	7.375

the atomic coordinates are listed in Table VII. The comparison of calculated and observed structure factor amplitudes have been deposited*. A projection and a stereoview of the unit cell are shown in Fig. 3.

CONCLUSIONS

A comparison of the structures of (1→3)-α-D-mannan and the corresponding glucan[7] reveals both considerable similarities and some differences. Among the

* The list of observed and calculated structure factor amplitudes can be obtained on request from Elsevier Scientific Publishing Company, BBA data Deposition, P.O. Box 1527, Amsterdam, The Netherlands. Reference should be made to No. BBA/DD/496/*Carbohydr. Res.*, 229 (1991) 57–74.

similarities it is evident that the two-fold helical chain conformation of the glucan, which is stabilized by the O-2 · · · O-4′ intramolecular hydrogen bond, is conserved in the mannan even though the same hydrogen bond cannot form. The similarities extend to such structural parameters as the glycosidic bridge angle and the glycosidic rotation angles ϕ and ψ. (It may be noted that the ϕ, ψ-angles observed here are very close to those present in the crystal structure of α-Man-(1→3)-α-Man-(1→4)GlcNAc[25] ($\phi = -58°$, $\psi = -19°$, as well as the minimum energy region predicted for this linkage by molecular mechanics calculations[26].) These common features support the notion that the chain conformation in polysaccharides tends to be governed more by its type of linkage rather than the residue. In this case, even the intramolecular hydrogen bond does not seem to have an important role in establishing the chain conformation.

Consistent with the crystal structures of other regenerated polysaccharides, (1→3)-α-D-mannan was also found to crystallize with antiparallel chain packing. This type of packing has now been found in all regenerated polysaccharide structures that crystallize in single-helical form, with linkage types[7,27–29] of α- and β-(1→3) and -(1→4). On the other hand, considerable differences in the chain packing of the mannan and the glucan are also evident. In the (1→3)-α-D-glucan[7] the chains pack into sheets along the *a*-direction of the unit cell and intermolecular hydrogen bonds develop both within and between the sheets. In contrast, as shown in the unit-cell projections of the mannan (compare Fig. 3), there is no apparent sheet-like packing of chains in this case. Along the *b*-axis of the unit cell, for example, the two chains of alternating polarity are not parallel with respect to the ring planes, which appears to prevent sheet formation in that direction. However, following the intermolecular hydrogen-bond scheme in the structure of mannan suggests reasons for the differing chain packing. As shown in Fig. 4, a series of two strong hydrogen bonds connect all four chains, running diagonally across the *ab*-plane through the unit cells, which results in an infinite zig-zag sheet of the chains. The water molecules, generally found between the sheets, provide

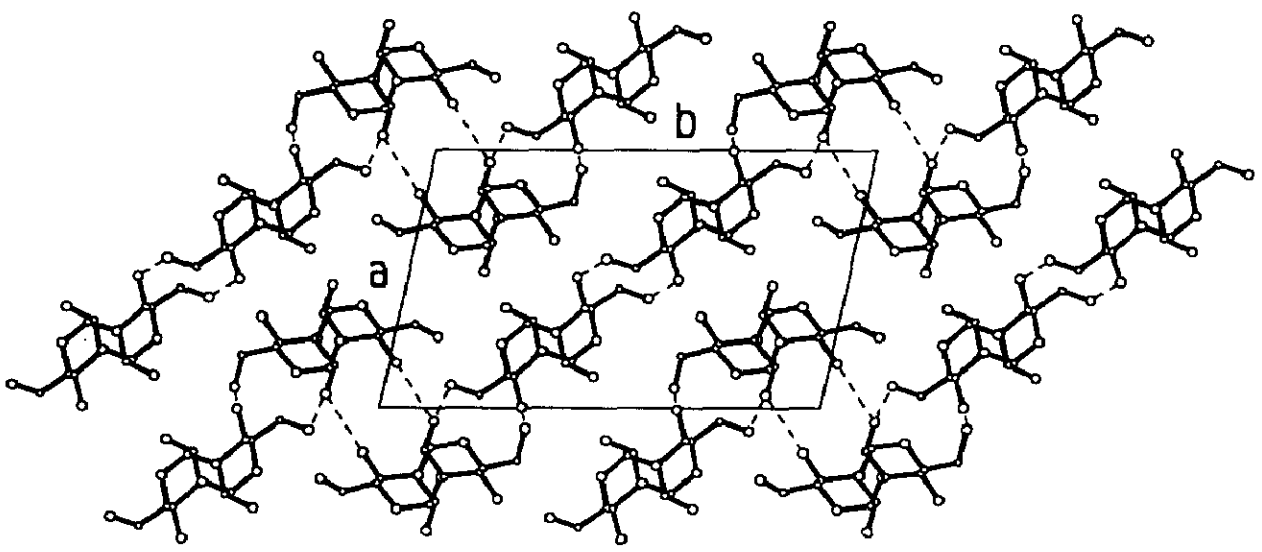

Fig. 4. Interchain hydrogen bonding sequences (shown by dashed lines) viewed as a projection on the *ab* plane.

additional hydrogen-bonding that clearly contributes to the extensive three-dimensional hydrogen-bond network in this crystal structure. These water molecules must reside firmly in their positions because it has been observed that evacuation does not convert the hydrate structure into the anhydrous form. A fiber pattern of the hydrate form was still obtained (albeit slightly more diffuse) from the sample in a vacuum at room temperature.

Despite the fact that similar conditions were used in preparing the regenerated forms of the (1→3)-α-D-glucan and the mannan, the former is anhydrous, while the latter is a hydrate. The corresponding β-(1→4)-linked regenerated glucan and mannan — crystallizing as cellulose II and mannan II — show similar hydration properties: cellulose II[27] exhibits a typical sheet structure, antiparallel chain packing, and is anhydrous. Mannan II, on the other hand, has been suggested to be a hydrate[30]. It is interesting that only the mannans and not the glucans have shown hydrate forms in their regenerated structures which are, presumably, energetically the most stable states. Whether the hydration is a peculiarity in the crystallization of the mannans or is a function of the chemical structure, is unknown. It would be of interest to determine the detailed crystal structure of mannan II for further comparison of these structures.

ACKNOWLEDGEMENTS

This work was supported by the National Science Foundation, under grants DMB8320548 and DMB8703725. We would like to thank Professor S. Ukai of the Gifu Pharmaceutical University for supplying a sample of the partially *O*-acetylated linear (1→3)-α-D-mannan.

REFERENCES

1 Y. Sone, M. Kakuta, and A. Misaki, *Agric. Biol. Chem.*, 42 (1978) 417–425.
2 S. Ukai, S. Morisaki, M. Goto, T. Kiho, C. Hara, and K. Hirose, *Chem. Pharm. Bull.*, 30 (1982) 635–643.
3 S. Ukai, K. Hirose, T. Kiho, and C. Hara, *ibid.*, 25 (1977) 338–344.
4 M. Kakuta, Y. Sone, T. Umeda, and A. Misaki, *Agric. Biol. Chem.*, 43 (1979) 1659–1668.
5 C. Hara, T. Kiho, and S. Ukai, *Carbohydr. Res.*, 111 (1982) 143–150.
6 K. Ogawa, T. Miyanishi, T. Yui, C. Hara, T. Kiho, S. Ukai, and A. Sarko, *ibid.*, 148 (1986) 115–120.
7 K. Ogawa, K. Okamura, and A. Sarko, *Int. J. Biol. Macromol.*, 3 (1981) 31–36.
8 H.C.H. Wu and A. Sarko, *Carbohydr. Res.*, 61 (1978) 7–25; 27–40.
9 A. Imberty, H. Chanzy, S. Perez, A. Buleon, and V. Tran, *J. Mol. Biol.*, 201 (1988) 365–378; A. Imberty and S. Perez, *Biopolymers*, 27 (1988) 1205–21.
10 R.H. Marchessault and Y. Deslandes, *ibid.*, 75 (1979) 231–242.
11 H. Nishimura and A. Sarko, *Macromolecules*, 24 (1991) 771–778.
12 A. Sarko, LSQ (*Fortran least-squares curve resolution program*); SUNY College of Environmental Science and Forestry, Syracuse, NY.
13 A. Sarko, FIBRXRAY (*Fortran X-ray intensity correction program*); SUNY College of Environmental Science and Forestry, Syracuse, NY.
14 R.E. Franklin and R.G. Gosling, *Acta Crystallogr.*, 6 (1953) 678–681.

15 A. Sarko and P. Zugenmaier, PS79 (*Fortran virtual bond structure refinement program*); SUNY College of Environmental Science and Forestry, Syracuse, NY.
16 P. Zugenmaier and A. Sarko, *ACS Symp. Ser.*, 141 (1980) 225–237.
17 C. Woodcock and A. Sarko, *Macromolecules*, 13 (1980) 1183–1187.
18 S. Arnott and W.E. Scott, *J. Chem. Soc., Perkin Trans. 2*, (1972) 324–335.
19 G.A. Jeffrey, R.M. McMullan and S. Takagi, *Acta Crystallogr., Sect. B*, 33 (1977) 728–737.
20 A. Sarko and R.H. Marchessault, *J. Polym. Sci., Part C*, 28 (1969) 317–331.
21 C.T. Chuah, A. Sarko, Y. Deslandes, and R.H. Marchessault, *Macromolecules*, 16 (1983) 1375–1382.
22 D.M. Lee and J. Blackwell, *Biopolymers*, 20 (1981) 2165–2179.
23 R. Moorhouse, W.T. Winter, S. Arnott, and M.E. Mayer, *J. Mol. Biol.*, 109 (1977) 373–391.
24 W.T. Winter and S. Arnott, *ibid.*, 117 (1977) 761–784.
25 V. Warin, F. Baert, R. Fouret, G. Strecker, G. Spik, B. Fourner, and J. Montreuil, *Carbohydr. Res.*, 76 (1979) 11–22.
26 A. Imberty, V. Tran, and S. Perez, *J. Comp. Chem.*, 11 (1989) 205–216.
27 A.J. Stipanovic and A. Sarko, *Macromolecules*, 9 (1976) 851–857.
28 W.T. Winter and A. Sarko, *Biopolymers*, 13 (1974) 1447–1460.
29 G. Rappenecker and P. Zugenmaier, *Carbohydr. Res.*, 89 (1981) 11–19.
30 E. Frei and R.D. Preston, *Proc. Roy. Soc. London, Ser. B*, 169 (1968) 127–145.